Int. J. Multiphase Flow Vol. 15, No. 5, pp. 815–829, 1989
Printed in Great Britain.
0301-9322/89 $3.00 + 0.00

CONTINUOUS SEPARATION OF BIDISPERSE SUSPENSIONS IN INCLINED CHANNELS

J. H. MASLIYAH, H. NASR-EL-DIN† and K. NANDAKUMAR
Department of Chemical Engineering, University of Alberta, Edmonton, Alberta T6G 2G6, Canada

(*Received* 27 *July* 1988; *in revised form* 13 *March* 1989)

Abstract—An experimental study was conducted to evaluate the enhancement for the continuous separation of light and heavy particles in an inclined column. A bidisperse suspension consisting of polystyrene (light) and polymethyl methacrylate (heavy) beads of respective uniform size and density, suspended in a salt solution, was used. The total solids volume fraction did not exceed 0.18 to insure uniform lateral concentration profile. The effects of feed flow rate, feed total solids concentration, feed composition, angle of inclination and split ratio on the recovery and on the purity of both species in the overflow and underflow streams were examined. The split ratio is defined as the ratio of the underflow volumetric flow rate to that of the feed. At a fixed feed flow rate, there is a threshold split ratio, beyond which the recovery drops linearly with increasing the split ratio. The threshold split ratio was found to be a function of the operating conditions. At a fixed set of operating conditions, increasing the angle of inclination results in a greater degree of separation. At a given split ratio, there is an optimum feed flow rate beyond which the enhancement decreases as the feed flow rate increases. A mathematical model based on the continuity equations and the PNK concept has been developed that predicts adequately the experimental measurements.

Key Words: inclined plate settlers, solids separation, bidisperse suspensions

INTRODUCTION

Separation of light and heavy particles from a suspension is encountered in many industrial applications, e.g. separation of heavy oil from oil–sand–water suspensions (Carrigy 1963). Enhancement in the settling rates of suspensions can be achieved by using an inclined container. This enhancement was originally observed by Boycott (1920) and is normally referred to as the *Boycott* effect. Settling in inclined channels has been studied extensively in recent years. Recent reviews on previous work have been given by Acrivos *et al.* (1983) and Davis & Acrivos (1985). Ponder (1925) and Nakamura & Kuroda (1937) were the first to explain enhanced settling rates in inclined channels based on kinematic and geometrical arguments. According to their model, the settling rate (i.e. the suspension–clear fluid interface velocity) in an inclined channel is given by

$$V = V_0\left(1 + \frac{H}{b}\sin\theta\right), \qquad [1]$$

where V is the settling rate in an inclined container, V_0 is the settling rate in a vertical container, H is the vertical height of the suspension, b is the spacing between the plates and θ is the angle of the inclination from the vertical. The presence of sediment is not taken into account in the above development. The validity of [1] was examined by various investigators. The predictions based on [1] have been found (Acrivos & Herbolzheimer 1979; Leung 1983) to be adequate in providing an upper bound on the settling rate. Various empirical modifications were introduced into [1] to obtain a better fit with the experimental measurements (e.g. Graham & Lama 1963; Vohra & Ghosh 1971). However, these models require some constants to be determined experimentally.

Acrivos & Herbolzheimer (1979) were first to identify the conditions for which [1] is valid. According to Acrivos & Herbolzheimer, [1] can be used to predict settling rate in inclined channels provided that: (1) the suspension is monodisperse; (2) the initial concentration distribution is uniform; (3) the particle Reynolds number is small; (4) Λ, the ratio of the sedimentation Grashof

†Petroleum Recovery Institute, Calgary, Alberta T2L 2A6, Canada.

number and the sedimentation Reynolds number, R, is large; and (5) the interface between the clear fluid and the suspension remains stable. Λ and R are defined as follows:

$$\Lambda = \frac{H^2 g(\rho_s - \rho_f)C_0}{V_0 \mu_f} \quad \text{and} \quad \mathrm{R} = \frac{\rho_f H V_0}{\mu_f}, \qquad [2]$$

where ρ_s and ρ_f are the solids and fluid densities, respectively, μ_f is the fluid viscosity, H is the suspension height, g is the gravitational acceleration and C_0 is the suspension solids concentration.

Interfacial instability in the form of waves can cause a discrepancy between the experimental measurements and predictions based on the PNK model. Herbolzheimer (1983) used a linear stability analysis to study these instabilities. According to his analysis, the maximum amplification of the interfacial waves occurs when the angle of inclination lies in the range of 10°–15°. Interfacial instabilities were also observed in continuous settling of monodisperse suspensions in inclined channels by Shaqfeh & Acrivos (1987).

Settling of polydisperse suspensions in inclined channels containing particles heavier than the fluid has been studied by Davis *et al.* (1982) and Schaflinger (1985). Schaflinger has shown that settling of polydisperse suspensions under moderate Re can lead to resuspension of the particles, resulting in departure from the PNK model.

Probstein *et al.* (1977) studied theoretically continuous separation of monodisperse suspensions in inclined columns with top-feeding. They observed two steady-state modes of operation: a subcritical mode where the feed layer expands down the channel; and a supercritical mode where it contracts. Probstein & Hicks (1978) were the first to verify the existence of these modes experimentally. Leung & Probstein (1983) studied the operating modes of inclined settlers using various feed locations. They only observed one mode of operation (subcritical) for bottom and middle feeding. Leung & Probstein also observed that the efficiency of the settler decreases as the solids concentration increases or the angle of inclination from the vertical decreases. Herbolzheimer & Acrivos (1981) examined settling in narrow inclined channels. They confirmed the existence of two steady-state modes of operation for top-feeding.

Batch separation of bidisperse suspensions having light and heavy particles has been examined by Law *et al.* (1987, 1988). In the absence of lateral concentration heterogeneities (fingers), it was found that the PNK model predicts the settling rates of the light and heavy particles fairly well. Nasr-El-Din *et al.* (1988) measured the exit concentrations of bidisperse suspensions in a *vertical* column under a continuous mode of operation. A theoretical model based on the continuity equation and the relative velocity was found to be adequate in predicting the performance of the vertical settler.

The objectives of the present work are: (1) to examine the effects of the operating conditions on the recoveries and the concentrations of the light and heavy particles in the product streams; and (2) to predict the concentrations in the product streams by using the PNK approach.

MATHEMATICAL MODEL

Modeling of the separation process of polydisperse systems in an inclined parallel plate container can be made either by using a kinematic approach, as was illustrated by the PNK model for batch settling of monodisperse suspensions, or by solving the momentum equations pertaining to the suspension, as was illustrated by Hill *et al.* (1977). The latter approach is quite complex for a bidisperse system undergoing separation in a continuous mode.

The model developed here assumes that the inclined parallel-plate gravity settler consists of a uniform source zone extending to the full length of the settler, as shown in figure 1. An interface between the source zone and the upper wall, denoted as interface 4, demarcates the fast rising convection current II and the suspension zone. The convection current is confined to a narrow region close to the plate and consists of fluid and light particles. A similar current I, moving downward and carrying fluid and heavy particles, is demarcated from the suspension zone by interface 3.

The overflow stream consists of the fluid, heavy and light particles crossing interface 2 together with the fluid and the light particles crossing interface 4. The underflow stream is supplied by the fluid, the heavy and light particles leaving interface 1 together with the fluid and heavy particles

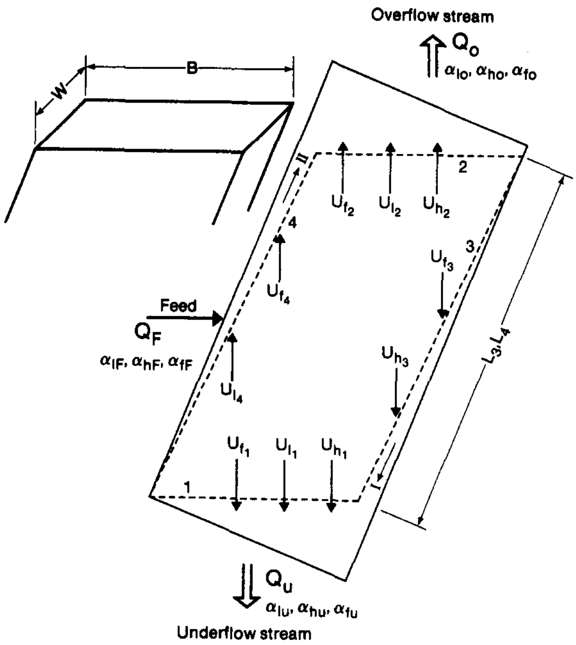

Figure 1. Schematic of the inclined settler for the mathematical model.

crossing interface 3. The light particles can only leave the source zone via interface 1 if the downward fluid velocity exceeds the rise velocity of the light particles; otherwise, its velocity is zero. Similarly, the heavy particles can only leave the source zone via interface 2 if the upward fluid velocity exceeds the settling velocity of the heavy particles. In this way, particles can only leave the source zone via the interfaces and no particles are allowed to enter the source zone except through the feed stream.

The fluid volumetric flow rate at the interface 4 is due to the volumetric settling rate of the heavy particles crossing interface 3. This concept is based on the PNK model as applied to monodisperse suspensions. Similarly, the downward fluid volumetric flow rate crossing interface 3 is due to the volumetric flow rate of the light particles crossing interface 4.

Taking the downward direction as positive, the volumetric balances over the source zone are given by the following equations.

Fluid

$$Q_F\alpha_{fF} = A_1 U_{f1}\alpha_f - A_2 U_{f2}\alpha_f + A_3 U_{f3}\alpha_f \sin\theta - A_4 U_{f4}\alpha_f \sin\theta, \qquad [3]$$

where U_{fi} is the vertical fluid velocity crossing interface i, α_f is the fluid volume fraction in the source zone and θ is the angle of inclination from the vertical. The areas A_j ($i = 1$ to 4) are given by

$$A_1 = A_2 = \frac{BW}{\cos\theta}$$

and

$$A_i = WL_i \qquad \text{for } i = 3 \text{ and } 4;$$

W is the settler depth and B is the width of the settler. L_3 and L_4 represent the lengths of the bidisperse zone, as shown in figure 1. Q_F is the feed volumetric flow rate and α_{fF} is the volume fraction of the fluid in the feed.

Light particle species

$$Q_F\alpha_{lF} = A_1 U_{l1}\alpha_l - A_2 U_{l2}\alpha_l - A_4 U_{l4}\alpha_l \sin\theta, \qquad [4]$$

where U_{l1}, U_{l2} and U_{l4} are the light particle species vertical velocities with respect to a stationary observer crossing the interfaces 1, 2 and 4, respectively. α_{lf} and α_l are the volume fractions of the light particle species in the feed and in the source zone, respectively.

Heavy particle species

$$Q_F \alpha_{hF} = A_1 U_{h1} \alpha_h - A_2 U_{h2} \alpha_h + A_3 U_{h3} \alpha_h \sin\theta, \qquad [5]$$

where U_{hi} is the heavy particle species vertical velocity with respect to a stationary observer at interface i. α_{hF} and α_h are the volume fractions of the heavy particle species in the feed and in the source zone, respectively.

The various volume fractions in the source zone are related by

$$\alpha_l + \alpha_h + \alpha_f = 1. \qquad [6]$$

For a given particle species, the relative velocity is given by Masliyah (1979) as:
heavy,

$$U_{hi} = U_{fi} + K_{hi}, \qquad i = 1 \text{ and } 3, \qquad [7a]$$

$$U_{hi} = \min[0, U_{fi} + K_{hi}], \qquad i = 2; \qquad [7b]$$

and

light,

$$U_{li} = U_{fi} + K_{li}, \qquad i = 2 \text{ and } 4, \qquad [8a]$$

$$U_{li} = \max[0, U_{fi} + K_{li}], \qquad i = 1; \qquad [8b]$$

where

$$K_{hi} = \frac{g(\rho_{hi} - \rho_s) d_h^2}{18\mu_f(1 + 0.15\mathrm{Re}_{hi}^{0.687})} \alpha_f^m, \qquad i = 1, 2 \text{ and } 3, \qquad [9]$$

and

$$K_{li} = \frac{g(\rho_{li} - \rho_s) d_l^2}{18\mu_f(1 + 0.15\mathrm{Re}_{li}^{0.687})} \alpha_f^m, \qquad i = 1, 2 \text{ and } 4, \qquad [10]$$

μ_f is the fluid viscosity and ρ_s is the source zone suspension density, given by

$$\rho_s = \alpha_l \rho_l + \alpha_h \rho_h + \alpha_f \rho_f. \qquad [11]$$

Re_{li} and Re_{hi} are the light and heavy particle species Reynolds numbers at interface i and they are given by Wallis (1969) as

$$\mathrm{Re}_{li} = |U_{li} - U_{fi}| d_l \alpha_f \frac{\rho_f}{\mu_f}, \qquad i = 1, 2 \text{ and } 4 \qquad [12]$$

and

$$\mathrm{Re}_{hi} = |U_{hi} - U_{fi}| d_h \alpha_f \frac{\rho_f}{\mu_f}, \qquad i = 1, 2 \text{ and } 3. \qquad [13]$$

ρ_f, ρ_h and ρ_l are the densities of the fluid, heavy and light particles, respectively. d_l and d_h are the mean diameters of the light and heavy particles, respectively. The parameter m is related to the Richardson & Zaki (1954) exponent, n, where $m = n - 2$ (Masliyah 1979). The exponent n is a function of both the particle Re and the ratio of the particle diameter to the container diameter. Using the hydraulic diameter of the rectangular vessel, the value of n was corrected to account for the wall effect according to Richardson & Zaki (1954).

The fluid velocities U_{f3} and U_{f4} adjacent to the inclined interfaces between the source zone and the settler can be calculated as follows:

$$A_3 U_{h3} \alpha_h = -A_4 U_{f4} \alpha_f \qquad [14]$$

and

$$A_4 U_{l4} \alpha_l = -A_3 U_{f3} \alpha_f. \qquad [15]$$

In operating a continuous settler one needs to specify either the overflow or the underflow rate. The underflow rate (Q_u) is given by

$$Q_u = A_1[U_{f1}\alpha_f + U_{h1}\alpha_h + U_{l1}\alpha_l] + A_3[U_{f3}\alpha_f + U_{h3}\alpha_h]\sin\theta. \qquad [16]$$

For a given feed flow rate and composition and a specified underflow rate, [3]–[16] provide the necessary equations to solve for the unknowns α_f, α_h, α_l, U_{fi} (i = 1 to 4), U_{hi} (i = 1, 2 and 3) and U_{li} (i = 1, 2 and 4).

The model equations were solved using a Gauss–Seidel iterative method with an under-relaxation factor of 0.5. Once the source zone composition and the interface velocities are known, then it becomes possible to evaluate the volume fractions of the light and heavy particles in the overflow (α_{lo}, α_{ho}) and in the underflow (α_{lu}, α_{hu}) streams as follows:

$$\alpha_{lo} = -\frac{[A_2U_{l2}\alpha_l + A_4U_{l4}\alpha_l\sin\theta]}{Q_o}, \qquad [17]$$

$$\alpha_{ho} = -\frac{[A_2U_{h2}\alpha_h]}{Q_o}, \qquad [18]$$

$$\alpha_{lu} = \frac{[A_1U_{l1}\alpha_l]}{Q_u} \qquad [19]$$

and

$$\alpha_{hu} = \frac{[A_1U_{h1}\alpha_h + A_3U_{h3}\alpha_h\sin\theta]}{Q_u}. \qquad [20]$$

The fraction recovery of the light particles in the overflow stream and the heavy particles in the underflow stream are given as

$$R_{lo} = \frac{Q_o\alpha_{lo}}{Q_F\alpha_{lF}} \qquad [21]$$

and

$$R_{hu} = \frac{Q_u\alpha_{hu}}{Q_F\alpha_{hF}}. \qquad [22]$$

In this model, it is assumed that the source zone composition above and below the feed inlet are the same. Moreover, the interface areas A_3 and A_4 are assumed to be constant and independent of the feed flow rate and the split ratio (Q_u/Q_F). From the flow visualization shown in figure 3, it can be seen that these assumptions are particularly true at a split ratio of about 0.5. Although many simplifying assumptions are used, it will be shown at a later stage that the predictions based on the kinematic model presented here agree fairly well with the experimental results of this study.

EXPERIMENTAL STUDIES

The experiments were conducted in a settler of 8 × 0.53 × 40 cm inner dimensions. The settler was mounted on a steel stand that could be rotated from 0° to 90° from the vertical, as shown in figure 2. The loop had three sampling ports to measure the solids concentration in the overflow, underflow and feed streams. The bidisperse suspensions used in the present study consisted of light polystyrene particles (d_l = 0.0265 cm and ρ_l = 1050 kg/m^3) and heavy polymethyl methacrylate particles (d_h = 0.0261 cm and ρ_h = 1186 kg/m^3) in a salt solution (μ_f = 1.41 mPa s and ρ_f = 1120 kg/m^3). The density of the salt solution was adjusted such that the settling velocities of the light and heavy particles were equal in magnitude. Both particle species consisted of mono-sized particles and they were prepared following the procedure described by MacTaggart *et al.* (1988). The heavy particles were dyed with Rhodamine B to aid in flow visualization. A few drops of Triton X-100 was used as a wetting agent.

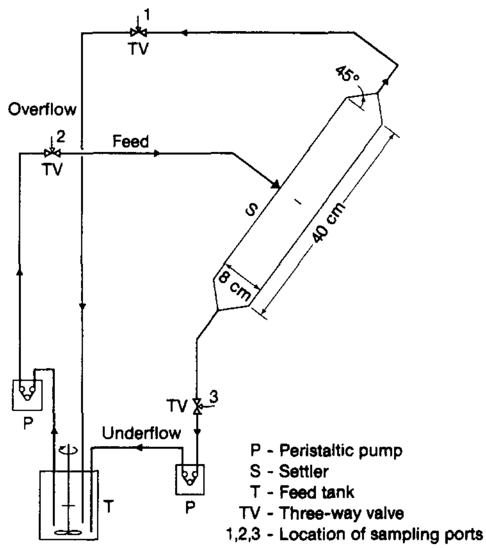

Figure 2. Experimental setup.

In each experiment the feed flow rate, Q_F, the feed compositions α_{lF} and α_{hF}, and the angle of inclination from the vertical, θ, were kept constant and the split ratio was varied from 0.1 to 0.9. The feed flow rate was varied form 1.4 to 4.3 cm^3/s. The angle of inclination from the vertical, θ, was varied from 0° to 45°. Three feed compositions were tested in this study: a symmetric feed of 6% light particles and 6% heavy particles; a symmetric feed of 9% light particles and 9% heavy particles; and an asymmetric feed of 3% light particles and 9% heavy particles. Experiments were conducted at a constant temperature of 20 ± 1°C. More details on the experimental procedure and sample processing are given elsewhere (Nasr-El-Din *et al.* 1988).

RESULTS AND DISCUSSION

Flow visualization

Figure 3a shows schematic diagrams for the flow patterns for a feed having α_{lF} and α_{hF} of 0.06 at $Q_F = 1.40$ cm^3/s. The angle of inclination of the settler is 30° from the vertical. Figure 3a-i shows the flow pattern at a split ratio of 0.2. One observes that the column has the following zones: (1) a bidisperse suspension in the upper half of the column and around the feed inlet; (2) a monodisperse heavy particle suspension in the lower half of the column; (3) a light sediment under the surface CDG, the thickness of this sediment increases as it approaches the overflow exit at point C; and (4) a heavy particle sediment above the surface BAF, the thickness of this sediment is minimum at point B and it reaches its maximum value above the surface AF. In addition to these zones, there are two convection currents: a descending current (I) begins at point B and it consists mainly of heavy particle suspension, and an ascending current (II) starts at point E and it consists of a clear fluid in the region that corresponds to the heavy particle suspension. As it approaches the bidisperse suspension zone, the fluid carries light particles and forms a monodisperse light suspension. Figure 3a-ii shows the various zones present for a split ratio of 0.5. One observes that by increasing the underflow flow rate, the size of the monodisperse heavy suspension zone and the clear fluid zone is decreased. Figure 3a-iii shows the flow pattern at a split ratio of 0.8. The dynamics of this case turns out to be a mirror image of figure 3a-i due to the symmetric nature of the properties of the fluid–particle system and the operating conditions. Figure 3a also shows that by increasing the split ratio (Q_u/Q_F), the amount of the heavy particle sediment decreases but the amount of the light particle sediment increases.

Figure 3b shows the flow patterns for a feed having $\alpha_{lF} = 0.03$ and $\alpha_{hF} = 0.09$ (i.e. feed total solids concentration of $\alpha_{tF} = 0.12$) at a feed flow rate of 1.40 cm^3/s. At a split ratio $Q_u/Q_F = 0.2$, the settler has the following zones: (1) a bidisperse suspension at the upper half of the settler; (2) a

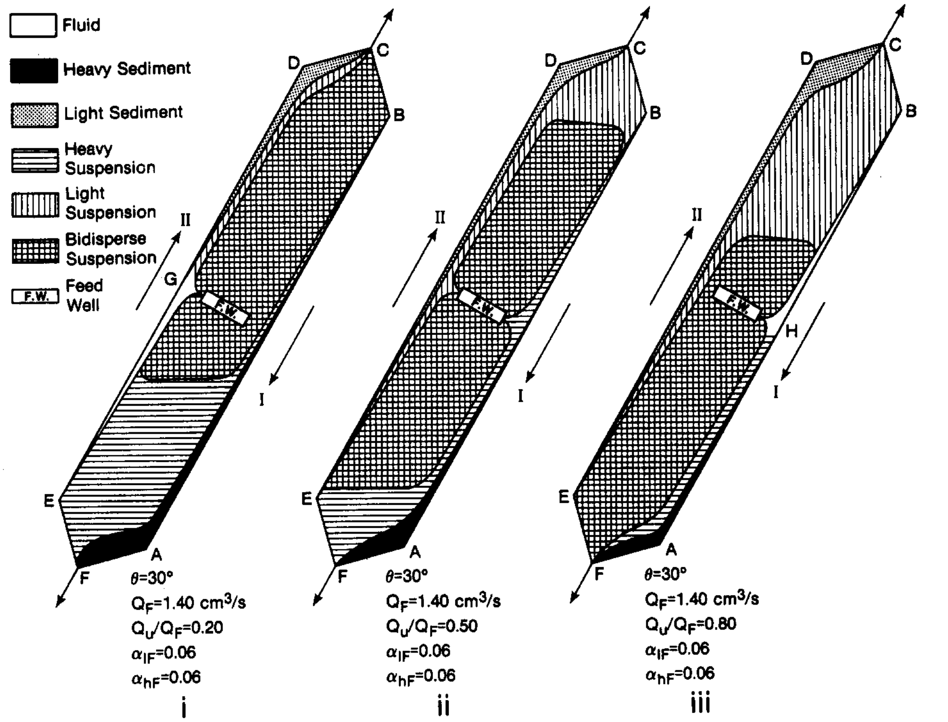

Figure 3a. Flow patterns for a feed having $\alpha_{lF} = \alpha_{hF} = 0.06$, $Q_F = 1.4\,\mathrm{cm^3/s}$ at $\theta = 30°$. (i) $Q_u/Q_F = 0.2$, (ii) $Q_u/Q_F = 0.5$, (iii) $Q_u/Q_F = 0.8$.

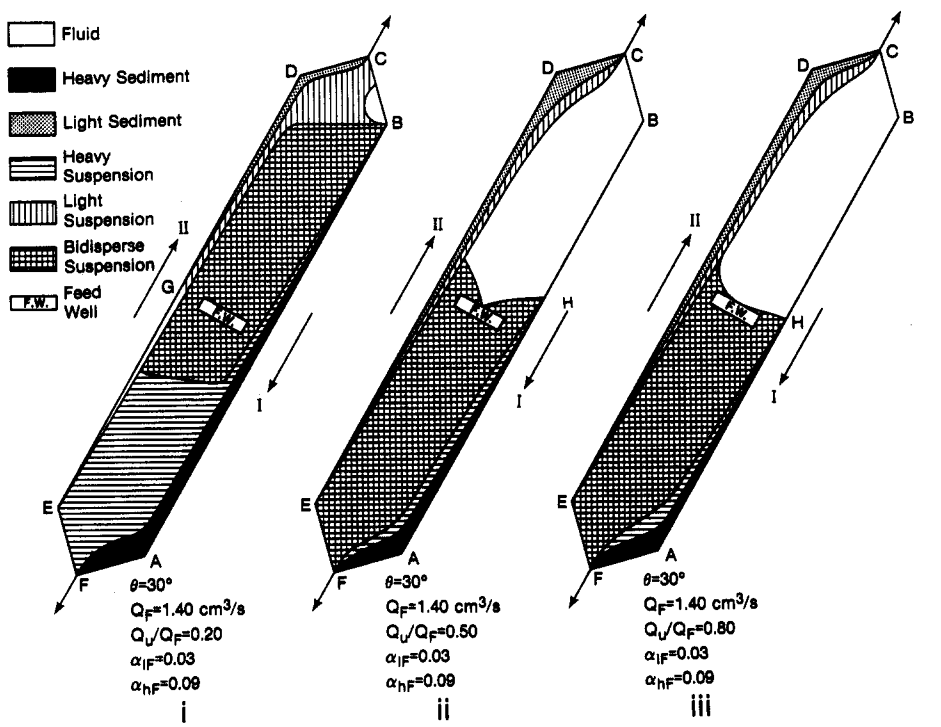

Figure 3b. Flow patterns for a feed having $\alpha_{lF} = 0.03$, $\alpha_{hF} = 0.09$, $Q_F = 1.4\,\mathrm{cm^3/s}$ at $\theta = 30°$. (i) $Q_u/Q_F = 0.2$, (ii) $Q_u/Q_F = 0.5$, (iii) $Q_u/Q_F = 0.8$.

monodisperse light particle suspension at the top of the column; (3) a monodisperse heavy particle suspension in the lower half of the column; (4) a small zone of trapped fluid beneath the surface BC; (5) a heavy particle sediment above the surface BAF; and (6) a light particle sediment below the surface CDG. The convection current (I) starts at point B and it consists of heavy particle suspension. The convection current (II) starts at point E and it consists of clear fluid. As the fluid passes the bidisperse suspension zone, it carries light particles and forms a light particle suspension. Figure 3b-ii shows the various zones at a split ratio of 0.5. One observes the clear fluid nearly occupies the upper half of the settler. The light particle suspension is limited to a narrow layer starting at point E. The bidisperse suspension zone lies only below the feed inlet. The convection current (I) starts at point H and it consists of heavy particles. Figure 3b-iii shows the flow pattern at a split ratio of 0.8. Basically, one observes the same zones noted at a split ratio of 0.5, but the size of the various zones is different. Here the size of the light particle sediment zone and that of the light particle suspension zone increases. The opposite trends occur for the corresponding zones of the heavy particles.

The flow patterns at various angles of inclination are basically similar to those shown in figures 3a and 3b. As the angle of inclination increases, the amount of light and heavy particle sediment increases. At an angle of inclination of 10°, both convection currents are wavy, indicating interfacial instabilities which were observed previously in batch settling of monodisperse (Herbolzheimer 1983) and bidisperse suspensions (Law *et al.* 1988) and continuous settling of monodisperse suspensions (Shaqfeh & Acrivos 1987). One also observes that the interfaces between monodisperse and bidisperse suspensions are horizontal. This is similar to batch settling of monodisperse suspension (Acrivos & Herbolzheimer 1979) and bidisperse suspensions (Law *et al.* 1988). Another important observation is that the mode of operation of this study is subcritical, which is the mode of operation for monodisperse suspension with a middle-feeding (Leung & Probstein 1983).

Effect of the split ratio

The effect of the split ratio is of interest because the fluid velocities in the upper and lower halves of the settler are functions of the split ratio. For a feed having particles of the same absolute settling velocities and same feed concentrations, one would expect the concentration of the light particles in one product stream to be equal to that of the heavy particle in the second product stream. Consequently, for such a case it is more convenient to combine the results as follows: the concentrations of the light species in the overflow and underflow streams are plotted against the split ratio Q_u/Q_F while those of the heavy particles are plotted as a function of Q_o/Q_F, or $(1 - Q_u/Q_F)$.

Figure 4 shows the effect of the split ratio on the concentrations of the light and heavy particles in the overflow and underflow streams at a feed flow rate of 2.85 cm^3/s and an angle of inclination of 10°. At split ratios $\leqslant 0.15$, the concentration of the light particles in the overflow, α_{lo}, is slightly higher than that in the feed, α_{lF}, and nearly zero in the underflow stream. This indicates that all the light particles in the feed are recovered in the overflow. At split ratios >0.15, the concentration of the light particles in the overflow and underflow streams increases as the split ratio increases. These results can be explained as follows: at low split ratios (Q_u/Q_F), the downward fluid velocity is not adequate to drag the light particles into the underflow stream and, consequently, the concentration of the light particles in the underflow is nearly zero. As the split ratio is increased, the downward fluid velocity increases. The fluid can drag the light particles into the underflow once the downward fluid velocity exceeds the rise velocity of the light particles. As a result of the higher downward fluid velocity, some of the light particles report to the underflow. The split ratio at which the light particles appear in the underflow or the heavy particles appear in the overflow will be referred to as the critical split ratio. The solid lines in figure 4 represent the model predictions, which agree well with the experimental results.

Effect of the angle of inclination

Figure 5 shows the variation of the light and heavy particles concentration in the product streams at $Q_F = 1.4\ cm^3/s$, with the angle of inclination as a parameter. As the angle of inclination is increased at a given split ratio, the concentration of the light particles in the overflow approaches $(Q_F\alpha_{lF}/Q_o)$; whereas the concentration of the light particles in the underflow stream approaches

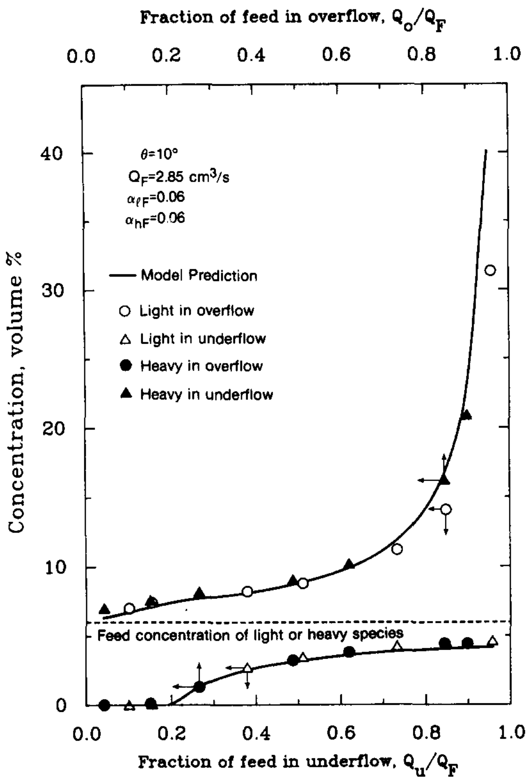

Figure 4. Variation of light and heavy particles concentration as a function of the split ratio for $\alpha_{lF} = \alpha_{hF} = 0.06$ and $\theta = 10°$.

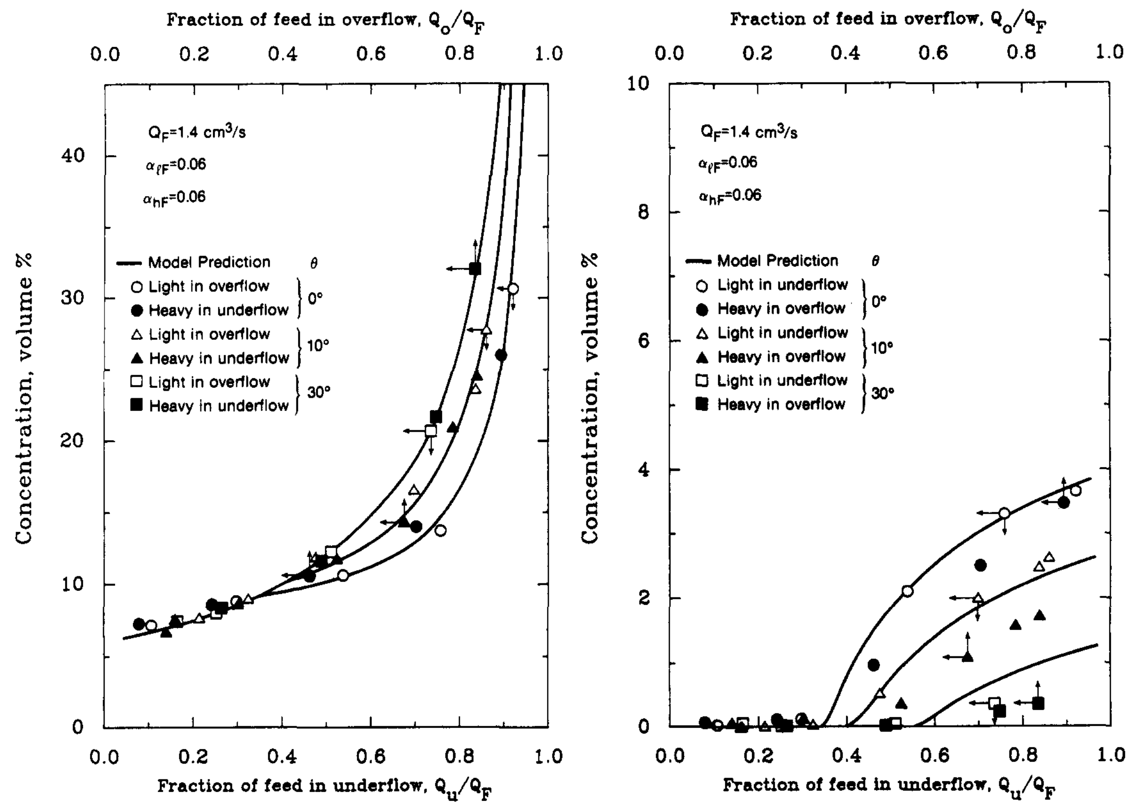

Figure 5. Variation of light and heavy particles concentration as a function of the split ratio for $\alpha_{lF} = \alpha_{hF} = 0.06$ and $Q_F = 1.40\ \text{cm}^3/\text{s}$.

zero. Similar trends occur for the concentrations of the heavy particles in the product streams. The critical split ratio is significantly reduced as the angle of inclination decreases. These results indicate that particle recovery can be improved using a continuous settler by increasing the angle of inclination from the vertical. This trend is similar to that observed in continuous separation of *monodisperse* suspensions (Leung & Probstein 1983).

Another measure to assess the performance of a settler is by examining the variation of the recovery (as defined in [21] and [22]) of one of the species as a function of the split ratio. Figures 6 and 7 show the variation of the recovery of the light particles in the overflow and heavy particles in the underflow as a function of Q_u/Q_F and $(1 - Q_u/Q_F)$, respectively, with the angle of inclination as a parameter. At low split ratios, the recovery of the light particles in the overflow stream is 100%. As the split is further increased, the recovery decreases linearly. It is useful to mention that a 100% recovery of light particles in the overflow only implies that all the light particles in the feed have been recovered in the overflow. In particular, it does not exclude the presence of any heavy particles in the overflow stream. One also observes that for a given split ratio, the recovery increases as the angle of inclination from the vertical increases. For all angles of inclinations examined, the recovery drops linearly as the split ratio increases beyond the corresponding critical split ratio. The limit of no separation implies that there is no differential settling in the column.

Effect of the feed flow rate

The effect of the feed flow rate on the performance of a settler is of interest since by increasing the feed rate the throughput increases, but the separation efficiency of the settler decreases. Figure 8 shows the variation of the light and heavy particles concentration in the product streams as a function of the split ratio at an angle of inclination of 30° from the vertical, with the feed flow rate as a parameter. For a given split ratio, as the feed flow rate is increased, the concentration of the light particles in the overflow and in the underflow streams approach that in the feed. One also notes that the critical split ratio (above which light particles appear in the underflow) is significantly decreased as the feed flow rate increases.

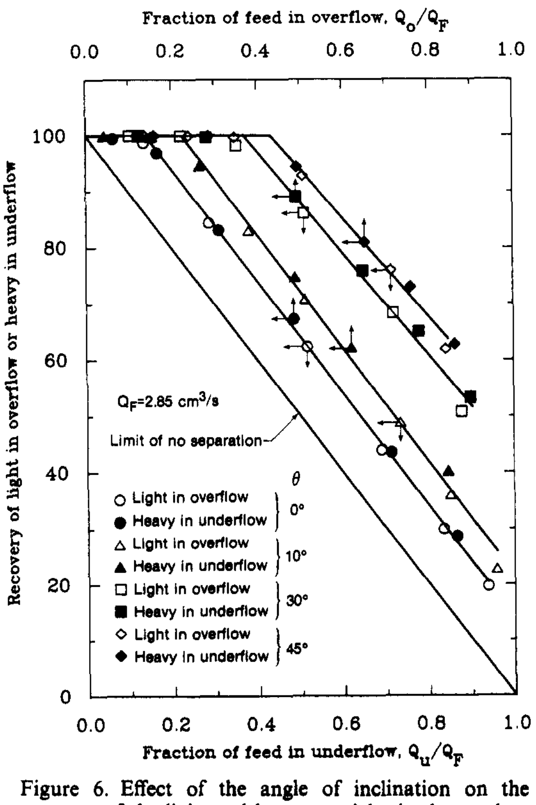

Figure 6. Effect of the angle of inclination on the recovery of the light and heavy particles in the product streams for $\alpha_{lF} = \alpha_{hF} = 0.06$ and $Q_F = 2.85\ cm^3/s$.

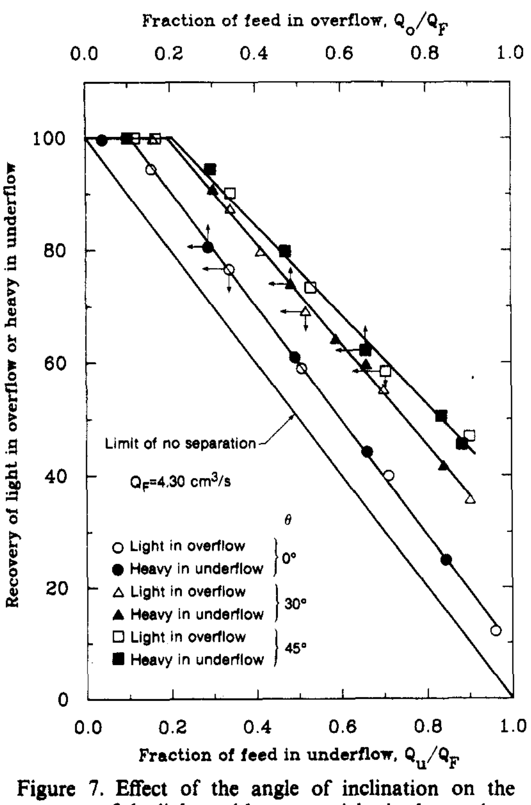

Figure 7. Effect of the angle of inclination on the recovery of the light and heavy particles in the product streams for $\alpha_{lF} = \alpha_{hF} = 0.06$ and $Q_F = 4.3\ cm^3/s$.

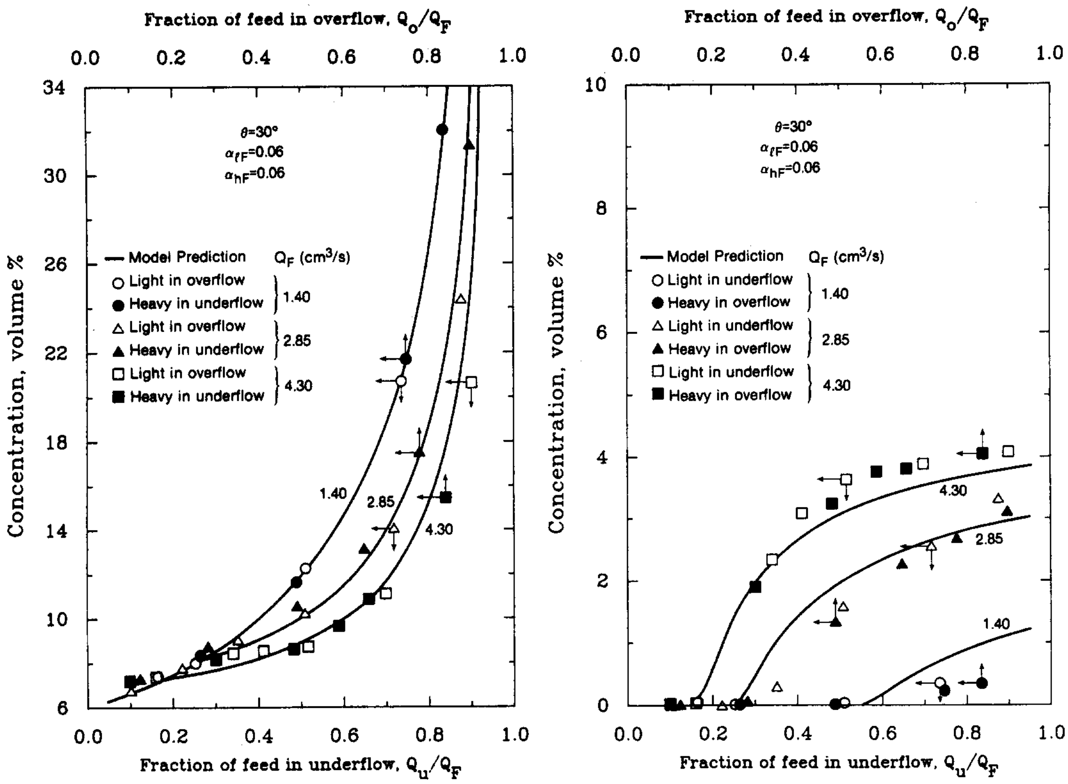

Figure 8. Effect of the feed flow rate on the light and heavy particles concentration in the product streams for $\alpha_{lF} = \alpha_{hF} = 0.06$ and $\theta = 30°$.

Figures 6 and 7 showed that the *recovery–split ratio* relationship is a function of the feed flow rate and the angle of inclination. Figure 9 shows the recovery enhancement factor as a function of the feed flow rate at a split ratio $Q_u/Q_F = 0.5$, with the angle of inclination as a parameter. The recovery enhancement factor is defined as the ratio of the recovery at an angle θ to that at angle $\theta = 0°$ (i.e. a vertical column) at the same conditions. For a given θ, the recovery enhancement factor curve exhibits a maximum, and both the location and the value of the maximum depend on the angle of the inclination. At very low feed flow rates, the settling process is 100% efficient at every angle and hence increasing the angle of inclination has almost no effect on the recovery.

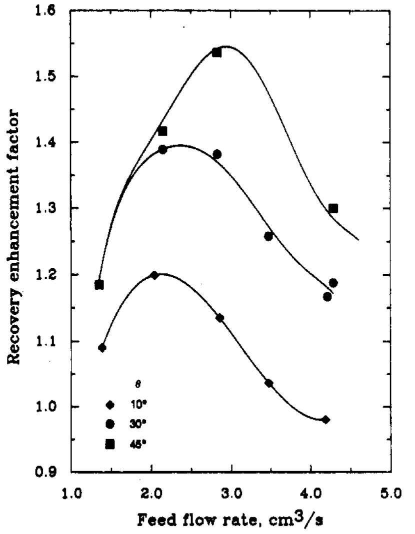

Figure 9. Effect of feed flow rate on the recovery enhancement factor.

Consequently, the recovery enhancement factor equals unity. At extremely high feed flow rates the settler efficiency approaches zero for all angles of inclination and, consequently, the recovery enhancement factor once again approaches unity.

Effect of the feed total solids concentration

The effect of the feed total solids concentration on the performance of the settler is of interest since particle settling velocity is a function of solids concentration. To examine this effect, the feed total solids concentration (α_{tF}) was raised to 18% ($\alpha_{lF} = \alpha_{hF} = 0.09$). This concentration was chosen as it is the highest concentration [based on our previous experiments with the same fluid–solids system in a batch mode, Law *et al.* (1988)] that can be used without the formation of lateral concentration variations (Whitemore 1955; Weiland *et al.* 1984).

Figure 10 shows the effect of the split ratio on the concentrations of the light and heavy particles in the overflow and underflow streams for $\theta = 30°$ at $Q_F = 1.40$ and $2.85\,\text{cm}^3/\text{s}$, respectively. Comparing figures 5 and 10 one observes the same trends on the variation of concentration (or purity) of product streams with changing split ratios and feed rates. The effect of α_{tF} on the performance of the column becomes clear by comparing the *recovery–split ratio* relationship, where the flow rate of any species in a product stream is normalized by the corresponding value in the feed. Figure 11 shows such a plot for two feed solids concentrations ($\alpha_{tF} = 0.12, 0.18$) at $Q_F = 1.4$ and $2.85\,\text{cm}^3/\text{s}$, respectively. For the case of lower feed flow, there seems to be a slight effect of the total feed concentration on the recovery of both species. A higher total feed solids concentration tends to give a lower value for the recovery. However, for the case of the higher feed flow rate, the effect of changing the total feed concentration has no influence on the recovery.

Effect of feed composition

Figures 12 and 13 show the concentrations of the light and heavy particles in the overflow and underflow streams as a function of the split ratio at an angle of inclination of 30°, with the feed

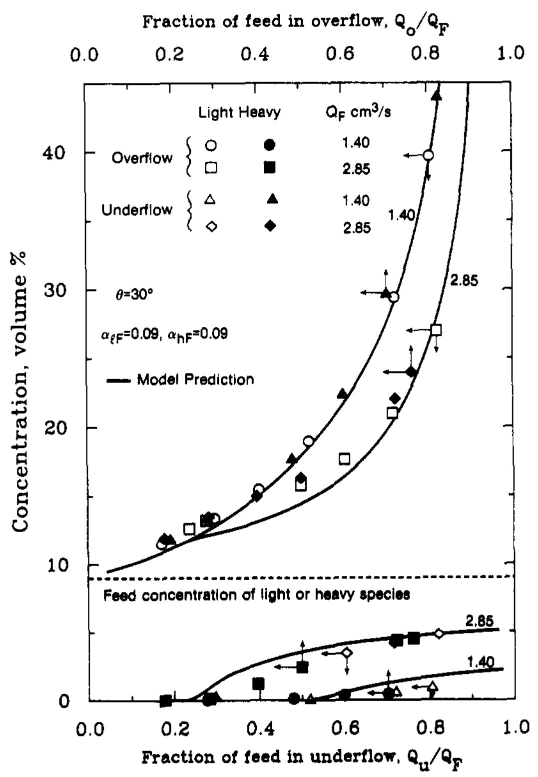

Figure 10. Variation of light and heavy particles concentration as a function of the split ratio for $\alpha_{lF} = \alpha_{hF} = 0.09$ and $\theta = 30°$.

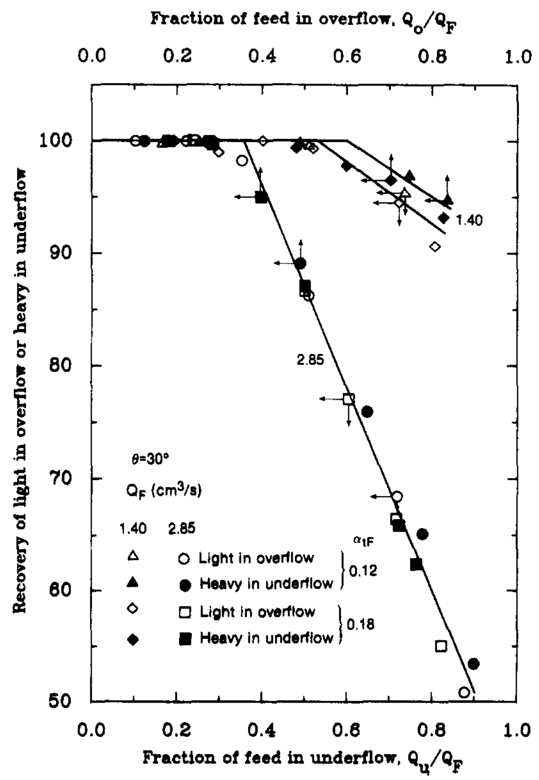

Figure 11. Effect of feed total solids concentration on the recovery in the product streams for $\theta = 30°$.

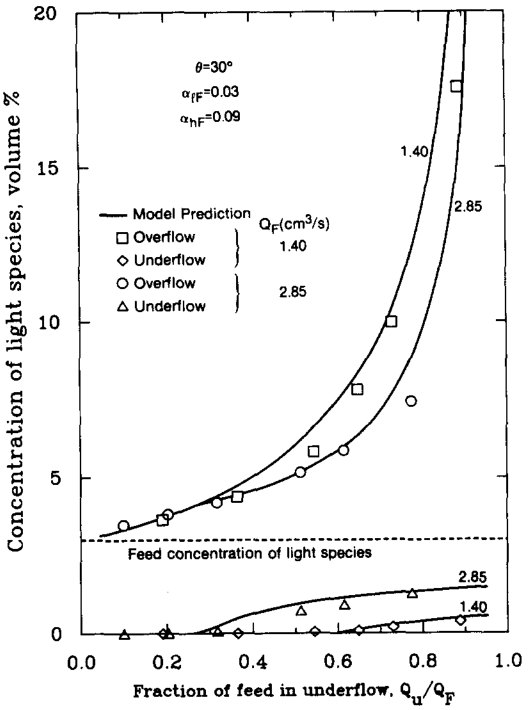

Figure 12. Variation of light particles concentration as a function of the split ratio for $\alpha_{lF} = 0.03$, $\alpha_{hF} = 0.09$ and $\theta = 30°$.

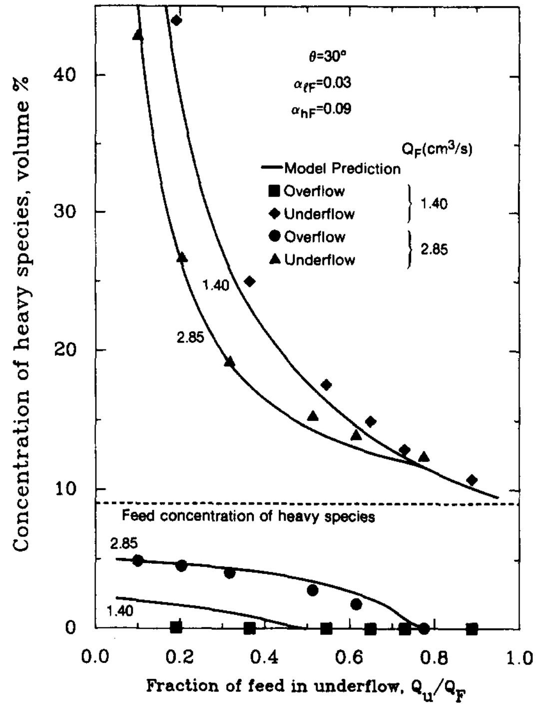

Figure 13. Variation of heavy particles concentration as a function of the split ratio for $\alpha_{lF} = 0.03$, $\alpha_{hF} = 0.09$ and $\theta = 30°$.

flow rate as a parameter for a feed composition of 3% light and 9% heavy particles. One observes that the concentrations of the light particles in the overflow and underflow streams are not symmetric to those of the heavy particles in the underflow and overflow, respectively. The effects of the split ratio and feed flow rate on the concentrations of both species in the product streams are similar to those obtained with a feed containing equal concentrations of light and heavy particles.

Figure 14 shows a comparison of the recovery of the light and heavy particles for a feed of 3% light and 9% heavy using a settler having an angle of inclination $\theta = 30°$ at a feed flow rate of 2.85 cm³/s. Unlike the recovery for symmetric feed shown in figures 6 and 11, the recovery of the light particles in the overflow is higher than that for the heavy particles in the underflow. The critical split ratio for the heavy particles is less than that of the light particles.

CONCLUSIONS

1. The degree of separation for the fluid–solids suspension examined in this study was found to be a function of the feed flow rate, feed total solids concentration, split ratio and angle of inclination. Increasing the feed flow rate, in general, results in decreased differential settling and hence poorer separation. Increasing the feed total solids concentration also results in lower recoveries due to hindered settling, especially at low feed flow rates.
2. The effect of the angle of inclination on the recovery of both species in the product streams was found to be significant. For a given split ratio, there is an optimum feed flow rate beyond which the recovery enhancement factor decreases as the feed flow rate increases.
3. For a given feed flow rate, there is a threshold split ratio beyond which the recovery drops linearly with increasing the split ratio. The threshold split ratio of a given particle species decreases as the feed flow rate, feed total solids concentration or its feed concentration increases.
4. A theoretical model developed using the PNK approach is adequate for predicting separation of light and heavy particles in a continuous inclined plate settler.

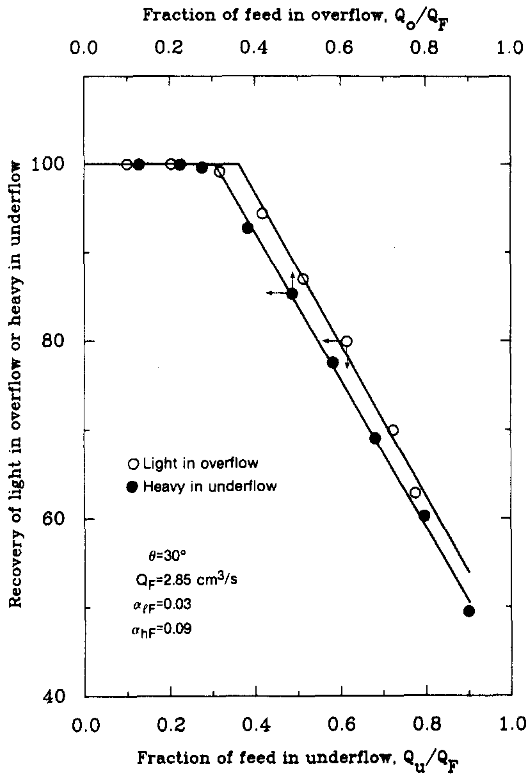

Figure 14. Recovery of the light and heavy particles in the product streams for $\alpha_{lF} = 0.03$, $\alpha_{hF} = 0.09$ and $\theta = 30°$.

Acknowledgement—This study was made possible through an Alberta Oil Sands Technology and Research Authority Contract (agreement No. 515) to K.N. and J.H.M.

REFERENCES

ACRIVOS, A. & HERBOLZHEIMER, E. 1979 Enhanced sedimentation in settling tanks with inclined walls. *J. Fluid Mech.* **92,** 435–457.

ACRIVOS, A., DAVIS, R. H. & HERBOLZHEIMER, E. 1983 Enhanced sedimentation in vessels having inclined walls: the Boycott effect. In *Theory of Dispersed Multiphase Flow* (Edited by MEYER, R. A.). Academic Press, New York.

BOYCOTT, A. E. 1920 Sedimentation of blood corpuscles. *Nature* **104,** 532.

CARRIGY, M. A. 1963 In *Athabasca Oil Sands* (Edited by CLARK, K. A.). Alberta Research Council, Edmonton.

DAVIS, R. H. & ACRIVOS, A. 1985 Sedimentation of noncolloidal particles at low Reynolds numbers. *A. Rev. Fluid Mech.* **17,** 91–118.

DAVIS, R. H., HERBOLZHEIMER, E. & ACRIVOS, A. 1982 The sedimentation of polydisperse suspensions in vessels having inclined walls. *Int. J. Multiphase Flow* **8,** 571–585.

GRAHAM, W. & LAMA, R. 1963 Sedimentation in inclined vessels. *Can. J. chem. Engng* **41,** 31–32.

HERBOLZHEIMER, E. 1983 Stability of the flow during sedimentation in inclined channels. *Phys. Fluids* **26,** 2043–2054.

HERBOLZHEIMER, E. & ACRIVOS, A. 1981 Enhanced sedimentation in narrow tilted channels. *J. Fluid Mech.* **108,** 485–499.

HILL, W. D., ROTHFUS, R. R. & LI, K. 1977 Boundary-enhanced sedimentation due to settling convection. *Int. J. Multiphase Flow* **3,** 561–583.

LAW, H. S., MASLIYAH, J. H., MACTAGGART, R. S. & NANDAKUMAR, K. 1987 Gravity separation of bidisperse suspensions: light and heavy particles species. *Chem. Engng Sci.* **42,** 1527–1538.

LAW, H. S., MACTAGGART, R. S., NANDAKUMAR, K. & MASLIYAH, J. H. 1988 Settling behavior of heavy and buoyant particles from a suspension in an inclined channel. *J. Fluid Mech.* **187,** 301–318.

LEUNG, W.-F. 1983 Lamella and tube settlers 2. Flow stability. *Ind. Engng Chem Process. Des. Dev.* **22,** 68–73.

LEUNG, W.-F & PROBSTEIN, R. F. 1983 Lamella and tube settler. 1. Model and operation. *Ind. Engng Chem. Process Des. Dev.* **22,** 58–67.

MACTAGGART, R. S., LAW, H. S., MASLIYAH, J. H. & NANDAKUMAR, K. 1988 Gravity separation of concentrated bidisperse suspensions in inclined plate settlers. *Int. J. Multiphase Flow* **14,** 519–532.

MASLIYAH, J. H. 1979 Hindered settling in a multi-species particle system. *Chem. Engng Sci.* **34,** 1166–1168.

NAKAMURA, H. & KURODA, K. 1937 La cause de l'acceleration de la vitesse de sedimentation des suspensions dans les recipients inclines. *Keijo J. Med.* **8,** 256–296.

NASR-EL-DIN, H., MASLIYAH, J. H., NANDAKUMAR, K. & LAW, H. S. 1988 Continuous separation of a bidisperse suspension in a vertical column. *Chem. Engng Sci.* **43,** 3225–3234.

PONDER, P. 1925 On sedimentation and rouleaux formation. *Q. Jl exp. Physiol.* **15,** 235–252.

PROBSTEIN, R. F. & HICK, R. E. 1978 Lamella settlers: a new operating mode for high performance. *Ind. Wat. Engng* **15,** 6–8.

PROBSTEIN, R. F., YUNG, D. & HICK, R. E. 1977 A model for lamella settler. In *Theory, Practice and Process Principles for Physical Separations*; *Proc. Engineering Foundation Conf.*, Asilomar, Calif., pp. 53–92.

RICHARDSON, J. F. & ZAKI, W. N. 1954 Sedimentation and fluidization: part I. *Trans. Instn chem. Engrs* **32,** 35–52.

SCHAFLINGER, U. 1985 Influence of nonuniform particle size on settling beneath downward facing walls. *Int. J. Multiphase Flow* **11,** 783–796.

SHAQFEH, E. S. G. & ACRIVOS, A. 1987 Enhanced sedimentation in vessels with inclined walls: experimental observations. *Phys. Fluids* **30,** 1905–1914.

VOHRA, D. K. & GHOSH, B. 1971 Studies of sedimentation in inclined tubes. *Ind. Engng Chem.* **13,** 32–40.

WALLIS, G. B. 1969, *One-dimensional Two-phase Flow*. McGraw-Hill, New York.

WEILAND, R. L., FESSAS, Y. P. & RAMARAO, B. V. 1984 On stabilities arising during sedimentation of two-component mixtures of solids. *J. Fluid Mech.* **42,** 383–389.

WHITEMORE, R. L. 1955 The sedimentation of suspensions of spheres. *Br. J. appl. Phys.* **6,** 239–245.